UC Santa Barbara

Title

Climate Change and Ground Water

Permalink

https://escholarship.org/uc/item/9f2615qw

Journal

Annals of the American Association of Geographers, 93(1)
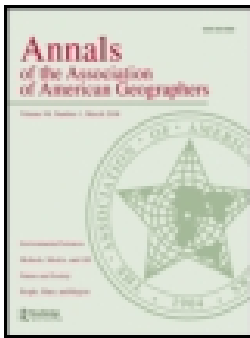
ISSN

2469-4452

Author

Loáiciga, Hugo A

Publication Date

2003-03-01

DOI

10.1111/1467-8306.93103

Peer reviewed

Climate Change and Ground Water

Hugo A. Loáiciga

Climate Change and Ground Water

Hugo A. Loáiciga

Department of Geography, University of California, Santa Barbara

This article summarizes the theory of climate change and the relationship of climate-change forcing to hydrologic and aquifer processes. It focuses on regional aquifer systems and on the methods to link large-scale climate-change processes to ground-water recharge and to simulate ground-water flow and solute transport in a warmer, $2xCO_2$ climate. The article reviews methods currently available to generate climate-change forcing and to simulate regional aquifer systems under ensuing hydrologic conditions. In addition, it outlines the development of a methodology to quantify the effects of climate change and of changes in ground-water use by population growth on hydrologic response. An example illustrates a specific procedure and our current capabilities and limitations to assess the potential impacts of a warming climate and population growth on regional-scale aquifer systems. The results indicate that aquifer exploitation strategies must take into account climatic variability and climate-change patterns. During protracted drought, the competition between human and ecological water uses is sharply accentuated. Changes in ground-water use may affect aquifer response more profoundly than climate change associated with modern global warming. *Key words: climate change, ground water, population.*

The Climate-Change Puzzle

What is climate change? The answer to this question, and a discussion of the effects that climate change might have on regional ground-water resources, constitutes the subject of this article.

For the purpose of current and future impacts, the term "climate change" has become synonymous with modern global warming (Demeritt 2001).[1] The latter, in turn, refers to post–Industrial Revolution changes in global mean surface-air temperature that are hypothesized to have been caused by increased atmospheric concentrations of carbon dioxide (CO_2)—an active greenhouse gas—during the eighteenth, nineteenth, and twentieth centuries. In 1765, the CO_2 atmospheric concentration was about 280 parts per million by volume (ppmv); in 2000, it is near 364 ppmv. The atmospheric concentrations of other greenhouses gases (methane, nitrous oxide, chlorofluorocarbons) have also risen as a result of accelerated economic activity and energy use in the last two centuries. The mean concentration of water vapor —another key greenhouse gas—in the atmosphere has remained at a level of about 3,000 ppmv throughout the Holocene period (the last 10,000 years).

The rapid rise in fossil-fuel combustion as an energy source since the late eighteenth century has caused the observed increase in the atmospheric concentration of CO_2. While the post–Industrial Revolution rise in CO_2 atmospheric concentration is beyond doubt, the question of whether or not the earth's mean surface-air temperature has increased relative to the pre–Industrial Revolution level is the focus of intense research. Recent estimates indicate that it has increased between 0.3°C and 0.6°C during the last 150 years (Intergovernmental Panel for Climate Change 2001; see Hansen et al. 2002 for other estimates). A cause-effect linkage between the rise in key greenhouse gases and the estimated increase in the global mean surface-air temperature remains shrouded in uncertainty. This is due to the complex variability of the earth's climate and its interdependence with multiple terrestrial and extraterrestrial phenomena (Loáiciga, Valdes et al. 1996).

Climate-Change and Hydrologic Scales

To the hydrologist, the question of whether or not global mean surface-air temperature has increased or will continue to increase, say, at a rate of 0.5°C every one hundred years is of secondary importance. The scope of the hydrologist's work is delimited by their capacity to measure hydrologic fluxes (water, substances, energy), to analyze them, and to make meaningful and useful inferences and predictions about them at relevant spatial scales. In the practical realm, where most hydrologic work lies, the intersection of hydrologically relevant spatial scales and administrative/political boundaries defines a clear context for the study of hydrologic processes, with or without climate change. Hydrologic studies are commonly restricted to the watershed and the regional aquifer system. Typically, this entails working with regions of less than 10^6 km^2, and in the great majority of cases the watershed or ground-water basin encloses areas well under 10^5 km^2 (Loáiciga 1997). These relevant spatial scales are

referred to in this work as "regional scales." Therefore, to the hydrologist, climate change must be resolved in terms of precipitation, surface-air temperature, evapotranspiration, sediment transport, ground-water levels, water quality, and runoff changes at the relevant spatial scales.

Hydrologic time-scales encompass a wide spectrum. In flood studies, the relevant temporal scales of precipitation range from minutes to days. In drought-impact studies, the precipitation and temperature temporal scales of interest vary from days to years, depending on the inter- and intraseasonal disposition of water in the natural and human-occupied environment (Loáiciga, Haston, and Michaelsen, 1993).

The remainder of this article provides a critical analysis of the state of the art in the analysis of climate change and its hydrologic consequences. The discussion focuses on the ground-water component of the hydrologic cycle, and one example is presented to illustrate the principles laid out in this work.

Climate-Change Predictions and Associated Hydrologic Consequences

Climate-Change Scenarios and Simulation Models

Early studies of the regional-scale hydrologic consequences of climate change, many produced between 1970 and the mid-1980s, were mostly based on simple scenarios for precipitation and temperature under a warmer climate (see Gleick 1989 for a review of representative articles). Precipitation was increased or decreased a certain percentage relative to historical values (the $\pm$ 10-percent range was commonly used). Historical temperature was increased a few degrees (typically between 1 and 5°C). With these two forcing variables, hydrologic models were then implemented to carry out simulations in the region of interest. The results thus obtained for important fluxes such as sediment output, ground-water recharge, and stream flow or other variables and water-resources systems of interest (e.g., ground-water levels, water-quality characteristics, reservoir storage and releases, irrigation scheduling, etc.) were compared with those that corresponded to the historical-climate simulations. The differences between the two sets of results were then attributed to climate change, all other things being equal (e.g., population, water use, cropping patterns, water technology).

A second wave of studies emerged in the refereed literature in the mid-1980s, based on the linkage between climate predictions from general circulation models (GCMs) and regional climate models (RCMs) (see Henderson-Sellers and Pitman 1992; Giorgi, Marinucci,

and Bates 1993a, 1993b; Giorgi, Shields-Brodeur, and Bates 1994; Vörösmarty et al. 2000). GCMs, which appeared in the global-scale climatic modeling community in the late 1960s, have been steadily improved in their physically based structure and numerical-solution algorithms. They have also evolved by incorporating refined spatial resolution of their numerical grids. RCMs have the same physical basis as GCMs but a much finer spatial resolution, and are confined to synoptic-scale and mesoscale simulation regions, rather than planet-wide simulations. At present, a GCM may have a spatial grid with cells on the order of 200 km $\times$ 200 km, while the RCMs have achieved resolutions on the order of 20 km $\times$ 20 km.[2] The RCMs rely on the coarser output from GCMs, which they use as initial and boundary conditions to drive their spatially refined simulations of climate change.

The great majority of GCM and RCM climate-change simulations are based on the so-called $2xCO_2$ scenario, whereby the 1990 CO_2 atmospheric concentration (about 355 ppmv, a base level adopted by the climate-change community; see, e.g., Houghton et al. 1996) is doubled and that value is used in the GCMs and RCMs to simulate the $2xCO_2$-warmer climate. The climate models simulate various climate-forcing variables of hydrologic interest at the land-atmosphere interface: precipitation, air temperature, radiant-energy fluxes, wind speed, atmospheric pressure, atmospheric humidity, latent-heat flux, and runoff averaged over the models' surface-grid cells. The RCMs' key output variables—such as precipitation, surface-air temperature, ground-level radiant-energy fluxes, water-vapor pressure, and wind speed—become the forcing input variables to hydrologic models, which then calculate, in a classical fashion, the dependent hydrologic variables of greatest interest, of which stream-flow and ground-water levels are examples. In some instances, GCMs and RCMs have undergone "subgrid" parameterizations that introduce approximate numerical representations of hydrologic processes at the land-surface interface, which allows them to make calculations of hydrologic fluxes at fine spatial resolution or at selected locations (e.g., at stream gauges or zones of influence of a water well). However, watershed-scale hydrologic models are better suited to carry out fine-resolution hydrologic simulations (e.g., of stream flows at selected gauges, spring flows, ground-water levels) due to their more realistic, physically based structure and internal parameterization (Panagoulia 1992; Vaccaro 1992). This is particularly true when attempting to simulate ground-water response to climate change, since ground-water flow, transport, and geochemical processes are poorly represented (if at all, as is the case with water-quality characteristics) by the subgrid
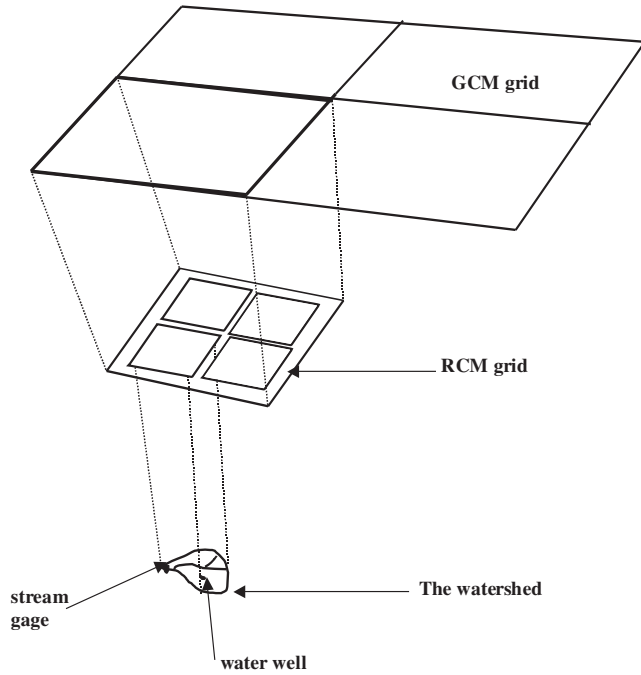
Figure 1. The nesting approach to simulate watershed-scale hydrologic fluxes in a warmer climate.

parameterizations thus far proposed. Thus, the GCM-RCM-hydrologic model linkage approach is the one pursued in this work. Figure 1 shows a graphical display of the "nesting" of hydrologic models within RCMs and of the latter within GCMs.

Climate-Scaling Factors and Hydrologic Simulation

The actual implementation of the nesting approach exemplified in Figure 1 may take several routes. One that has received considerable attention in the United States by the country's leading global-climate simulation agency, the National Center for Atmospheric Research (NCAR), relies on climate-scaling factors used in conjunction with historical climatic time series. Climate change is quantified in terms of scaling factors that involve $1xCO_2$ and $2xCO_2$ nested GCM/RCM-simulated forcing variables (e.g., temperature, precipitation, and runoff). The $1xCO_2$ nested GCM/RCM simulations correspond to the 1990 CO_2 atmospheric concentration.

Scaling factors are used in two ways to generate climate-change scenarios from historical time series. The first consists of multiplying a historical time series by the corresponding scaling factor (or, strictly speaking, scaling ratio in this case). Using precipitation (P) as an example, the equation used to generate the $2xCO_2$ precipitation

scenario is as follows:

$$P_{2xCO_2 \text{scenario}} = \frac{P_{2xCO_2}}{P_{1xCO_2}} \cdot P_{\text{historical}} \qquad (1)$$

If the nested GCM/RCM simulations of P_{1xCO_2} and P_{2xCO_2} are unbiased and independent estimators of precipitation under $1xCO_2$ and $2xCO_2$ conditions, respectively, then the expected value of the estimated precipitation $P_{2xCO_2 \text{scenario}}$ is equal to the $2xCO_2$ precipitation mean (μ_{2xCO_2})—that is, $P_{2xCO_2 \text{scenario}}$ is also an unbiased estimator. It is implied in the latter statement that $P_{\text{historical}}$ and P_{1xCO_2} have identical expected values that are both equal to the historical mean.

Temperature scaling is based on the difference between the $1xCO_2$ and $2xCO_2$ temperatures, $T_{2xCO_2} - T_{1xCO_2}$, which is applied to the historical temperature $(T_{\text{historical}})$. Specifically, the global-warming scenario $(T_{2xCO_2 \text{scenario}})$ is constructed according to the following equation:

$$T_{2xCO_2 \text{scenario}} = \{T_{2xCO_2} - T_{1xCO_2}\} + T_{\text{historical}} \qquad (2)$$

If T_{1xCO_2} and T_{2xCO_2} are unbiased estimators of temperature under $1xCO_2$ and $2xCO_2$ conditions, then the expected value of the estimated scenario $T_{2xCO_2 \text{scenario}}$ equals the $2xCO_2$ mean temperature—that is, $T_{2xCO_2 \text{scenario}}$ is also an unbiased estimator. This assumes that the expected values of T_{1xCO_2} and $T_{\text{historical}}$ are both equal to the historical mean temperature (that is, they are unbiased estimators).

The rationale behind the use of scaling factors is that, although nested GCM/RCM simulations may not accurately estimate the local statistics of regional climate variables, the models' internal consistency and physical basis may provide plausible estimates of the scaling ratios and differences. The climate scenarios generated with the scaling ratios and differences in combination with historical time series are then used to drive hydrologic and aquifer models, completing the nested simulation of hydrologic fluxes in a $2xCO_2$, warmer scenario.

The scaling factors have been developed for the conterminous United States as part of NCAR's Vegetation Ecosystem Modeling and Analysis Project (VEMAP) database, accessible online (see Kittel et al. 1995). The VEMAP database also contains historical times series (e.g., precipitation and temperature). Precipitation was measured at 8,500 stations and temperature at 5,500 stations in the United States. A kriging technique was applied to the historical data to yield estimates gridded at a $0.5°$ latitude $\times 0.5°$ longitude resolution. The derived $0.5° \times 0.5°$ gridded data set is a temporally complete (i.e., there are no data gaps in time) and geographically realistic representation of the historical climate record. The VEMAP database contains scaling factors for precipita-

tion and temperature (as well as for other climate variables) generated by seven leading GCMs nested within NCAR's RCM.

The 2xCO$_2$ climate scenarios created by means of the scaling approach are a function of historical events, and this constraint raises questions about the approach's suitability for predicting plausible climate-change forcing that might depart significantly from historical patterns. On the other hand, unconstrained simulation by GCMs and RCMs of a changing climate far into the future (commonly to 2050 or 2100) is bedeviled by the chaotic nature of climate predictions, which tend to diverge outside their probable range after a few years into a simulation (see Lorenz 1963, 1967; Kerr 1994, 1997; Loáiciga, Valdes et al. 1996).

On Climate-Hydrologic Feedbacks and 2xCO$_2$ Uncertainty

The chaotic nature of medium- and long-term climate predictions has already been mentioned. Small differences (say, a 1-percent difference) in the initial conditions of variables simulated by GCMs and RCMs lead to large divergence from and inaccuracy in their predicted values as time goes by—say, after ten or more years of simulation. The inability to predict the climate far into the future poses serious questions about model-simulated scenarios of 2xCO$_2$, given that the likelihood of reaching such an equilibrium level of atmospheric concentration does not seem feasible within the next one hundred years or even in the next few centuries.

Climate feedbacks constitute a second complication in the accurate simulation of 2xCO$_2$ or transient climate scenarios. Several authors have identified important feedbacks in the climate system that are not well-captured in GCMs and RCMs (see, e.g., Ramanathan and Collins 1992; Loáiciga, Valdes et al. 1996). Here, "feedback" means the interaction established between climate forcings (e.g., increased atmospheric opacity to Earth-emitted long-wave radiation) and the response of the terrestrial (and marine) environment, which acts to either accentuate or dampen those forcings. A positive feedback on surface temperature would act to increase it, while a negative would reduce it. The next section of this article reviews key climate feedbacks.

The Water-Vapor Feedback

The water-vapor feedback on climate is positive. Increased CO$_2$ concentrations produce larger infrared radiation to the Earth's surface, raising its temperature.

That rise in temperature evaporates more water, which raises atmospheric humidity. The evaporated water transfers latent heat to the atmosphere, which increases tropospheric temperature after the water vapor condenses. The greater tropospheric temperature enhances the water-holding capacity of the atmosphere, and hence its humidity. Water vapor, an effective greenhouse gas, traps Earth-emitted infrared radiation and, along with the warmer troposphere as a whole, increases infrared emissions back to the Earth's surface, heating it up further. Black-body cooling of the warmer surface-atmosphere system (i.e., by long-wave radiative emission to outer space according to the Stefan-Boltzmann law) impedes runaway warming of the earth's surface. In addition, the water-vapor (positive) feedback forcing has its own natural "brakes," such as the (negative) lapse-rate feedback (see Lindzen 1990).

The Cloud Feedback

In the present climate, in which the global mean cloudiness is 50 percent, clouds have both a positive forcing and a negative one. Positive climate forcing arises from the trapping of Earth-emitted infrared radiation, while the negative forcing is caused by the reflection of incoming solar radiation back to space, thereby reducing the flux of radiant energy reaching the surface compared to clear-sky areas. Earth-radiation studies seem to indicate that clouds have a net negative forcing that is responsible for a surface temperature between 10 and 15°C cooler than it would otherwise be (Ramanathan and Collins 1992). Most GCMs predict a decrease in global mean cloudiness in a warmer climate, in spite of the increased atmospheric humidity expected in that case. As a result, because of the strong albedo effect of clouds (i.e., they reflect incoming solar radiation), the overall predicted drop in cloudiness has a net positive (warming) feedback on the climate under the 2xCO$_2$ scenario, according to according to most GCMs.

Surface Albedo, Soil Moisture, and Vegetation Feedbacks

The surface albedo feedback refers mainly to ice-mass modifications in a warmer climate. A warmer climate, with surface temperatures magnified at high latitudes according to GCMs, melts ice and snow. These two surfaces are generally more reflective than water or land surfaces. Therefore, a warmer climate may reduce the surface planetary albedo (the ratio of reflected to incoming shortwave radiation), increasing the absorption of incom-

ing solar radiation. The latter effect warms the surface further, giving rise to the ice-albedo feedback.

The soil-moisture feedback is bound to occur in regions in which precipitation is predicted to decline, at least seasonally, such as during the summer in central North America. With lower precipitation and a warmer surface, the soil surface becomes drier. Evapotranspiration is reduced as the soil moisture drops. This reduces cloud formation. As evapotranspiration declines, so does the evaporative cooling associated with latent heat removal from the surface. Reduced cloud formation enhances surface warming as the atmosphere becomes less reflective to solar radiation. The reduced evaporative cooling and the enhanced atmospheric transparency start the soil-moisture feedback on surface warming, which is positive, according to this reasoning.

Vegetation feedbacks on climate are poorly understood. The vegetation feedback that results from surface warming may be triggered by changes in vegetated areas and in the type of vegetative cover. These changes can alter the surface-atmosphere temperature through modifications in the surface albedo and in the CO_2 exchange between the atmosphere and the earth's surface. Plant growth and respiration depend on atmospheric CO_2, surface temperature, and soil moisture. The interactions among these variables introduce several degrees of freedom and uncertainties in the biosphere-climate system. Under these circumstances, even the prediction of the sign of the vegetation feedback is highly uncertain.

The Aerosol Feedback

Aerosols (fine solid particles found in gaseous suspension in the atmosphere) introduce other complexities in the analysis of climate feedbacks. On the one hand, aerosols reflect incoming solar radiation, which would cause a negative climate feedback. On the other hand, they serve as cloud-formation nuclei, and clouds—depending on their particular characteristics—may induce either positive or negative climate feedbacks. A still-controversial clue about net aerosol feedback may be found in climate simulations. GCM predictions based on increased concentrations of greenhouse gases overestimate the global mean temperature in the post–Industrial Revolution era. Improved resemblance between the GCM-predicted and observed temperatures was achieved with the introduction of a negative radiative forcing attributed to sulfate aerosols in climate simulations (Mitchell et al. 1995). The technique used by those authors relied on adjusting the parameterization of surface albedo to account for the backscattering of solar radiation by sulfate aerosols. The ex post facto nature of the aerosol

fix for a GCM shortcoming has raised questions concerning circular logic in the restructuring and recalibration of climate models (Demeritt 2001). The role of aerosols in modern climate change continues to be actively assessed in the climate-research community (Forest et al. 2002).

Climate Change and Regional Ground-Water Systems

Ground-Water Recharge in the Hydrologic Cycle

Consider the hydrologic balance equation in a regional aquifer, in which R denotes natural ground-water recharge, G is the net ground-water flow in the aquifer, W is net withdrawal of ground-water by humans (+ represents an extraction, − an artificial recharge), and ΔS_G is the change of ground-water storage in the aquifer during a period of time (= the time step in hydrologic simulation):

$$\Delta S_G = R - G - W \qquad (3)$$

Climate change impacts ground-water systems through changes in aquifer recharge, while human-induced effects are reflected in the withdrawal term W. Ground-water recharge is determined by ground-water conditions, but also by the surface-water and the vadose-zone hydrologic balances. Let ET = evapotranspiration, P = effective precipitation, O = overland flow, ΔS_S = change in surface-water storage, I = infiltration, X = interflow (vadose-zone water flow to streams), and ΔS_V = change in the vadose-zone storage. The surface and vadose-zone water-balance equations are given by the following:

$$\Delta S_S = P - ET - O - I \qquad (4)$$

$$\Delta S_V = I - R - X \qquad (5)$$

Equations (3), (4), and (5) show how the water-storage status and fluxes in the land-surface, vadose-zone, and ground-water reservoirs are coupled. In order to discern the effect of climate change on ground-water recharge, one must also consider the changes in precipitation, evapotranspiration, infiltration, and the various components of total runoff (e.g., overland flow, interflow, baseflow), as well as the changes in water storages. This is possible only through the implementation of a continuous-time hydrologic simulation model that integrates land-atmosphere interactions and subsurface process.

Ground-Water Recharge Mechanisms

Natural ground-water recharge occurs by two main mechanisms. The first is spatially distributed recharge to the aquifer from the vadose zone (diffuse recharge; see

Stone, Moomaw, and Davis 2001 for a recent example). The second is seepage from streambeds and lake bottoms into the underlying aquifers. Local conditions determine the relative contributions of these two types of recharge mechanisms to the total ground-water recharge. Loáiciga (2000) and Loáiciga, Maidment, and Valdes (2000), for example, quantified the stream recharge in a regional-scale karst aquifer in which recharge occurred only in sections of stream channels that were hydraulically connected to the underlying water table. Everywhere else, the aquifer was isolated from the surface hydrologic cycle by impermeable strata. Thus, no diffuse recharge existed in that particular instance.

When stream recharge is the dominant mechanism of aquifer recharge, the linkage between climate-change forcing and aquifer response can be simplified. Linked GCM-RCM simulations can be used to generate stream-flow scaling factors Q_{2xCO_2}/Q_{1xCO_2} and then used to generate $2xCO_2$ ground-water recharge directly.[3] The historical recharge along a stream reach is given by the following stream-flow balance equation:

$$R_{historical} = Q_U + Q_I - Q_D \qquad (6)$$

where Q_U and Q_D are stream flows measured in the uppermost and lowermost channel cross sections in the recharge zone, respectively, and Q_I is the stream-flow contribution generated within the recharge zone itself. The right-hand side of Equation (6) involves stream-flow variables that can be scaled up by the runoff-scaling factors applicable to the area of interest. Specifically, the $2xCO_2$ aquifer recharge (R_{2xCO_2}) is given by the following expression:

$$R_{2xCO_2} = \frac{Q_{2xCO_2}}{Q_{1xCO_2}} R_{historical} \qquad (7)$$

$R_{historical}$ may be either monthly or annual recharge. The recharge from equation (7) is input to a ground-water simulation model to simulate $2xCO_2$ ground-water processes.

Approach and Example of Climate-Change Forcing in a Regional Aquifer

Steps to Assess Climate-Change Forcing of Aquifer Systems

This section illustrates the steps to analyze climate-change impacts in aquifer systems. The first step is to create the climate-change scenario. This could be as simple as specifying changes in precipitation (P) and temperature (T) — for example, 10 percent P increase and $+2°C$ T rise. When this simple method is used, the hydrologist commonly implements empirical evapotranspiration equations based on temperature (e.g., Thornthwaite's 1948 method or Hargreaves' method [see Hargreaves and Zamani 1982; Loáiciga, Maidment, and Valdes 2000). At the other extreme of complexity, GCMs or linked GCM-RCMs may be implemented to calculate the climate-change forcing. This can take the form of study-specific simulations or be based on the climate-scaling factors discussed above.

The second step is to estimate ground-water recharge under the climate-change scenario. The simplest method of doing this is to specify ground-water recharge as a fraction of precipitation, as was done by Loáiciga and Leipnik (2000). This simple method is best suited for ground-water simulations with annual time steps. For shorter time steps, the approach embodied by Equation (7) is particularly well suited for streambed recharge, provided that the runoff scaling factors are available. Otherwise, ground-water recharge must be calculated from hydrologic simulation driven by the climate-change forcing scenarios. If the hydrologic model features coupled surface-water/ground-water modules, then it can simulate the ground-water variables of interest, such as hydraulic heads, changes in ground-water storage, or chemical concentrations (if a water-quality module is available) and the analysis is, at that point, complete as far as climate-change/ground-water processes are concerned. Otherwise, the estimated ground-water recharge is used to drive a ground-water simulation model such as Modflow or a coupled ground-water/transport model such as Visual Modflow (Waterloo Hydrogeologic). Once the ground-water response to climate is calculated, it can be used in more complex water-resources assessments of climate change.

Recharge Dynamics in the Edwards Aquifer, Texas

The Edwards Balcones Fault Zone Aquifer system (henceforth the Edwards Aquifer) has been studied by Loáiciga, Maidment, and Valdes (2000) and Loáiciga (2000) from the viewpoint of climate change. The Edwards Aquifer is one of the most productive regional aquifers in the United States. It is the primary source of water (agricultural and municipal) in south-central Texas. The city of San Antonio, with a population in excess of one million people, relies on the Edwards Aquifer as its source of potable water. Figure 2 shows a map of the United States with an outline of the Edwards Aquifer system. The map depicts three river basins (Colorado River, Sacramento River, and the Apalachicola [ACF] River) that have been
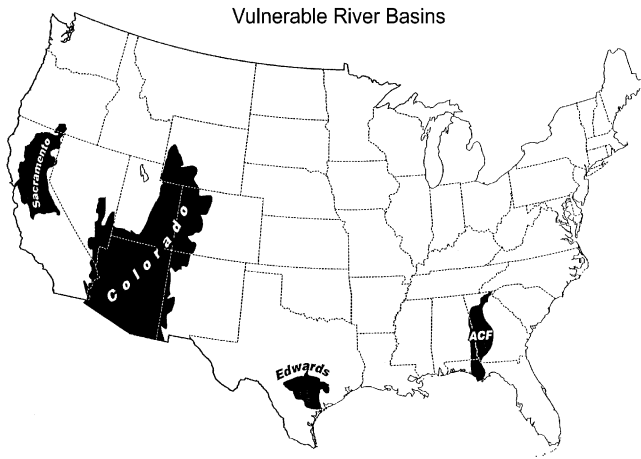
Figure 2. Edwards Aquifer and three river basins vulnerable to climate change in the United States.

classified, together with the Edwards Aquifer, as being very vulnerable to climate-change impacts (Loáiciga, Maidment et al. 1996). The Edwards Aquifer is unique among these threatened water systems in being the only underground water resource. It has also been considered to be the water basin in the United States most vulnerable to climate change according to a diverse set of vulnerability indicators (Loáiciga, Maidment et al. 1996).

The hydrogeologic features of the Edwards Aquifer have been described by Maclay and Small (1984), among others. It lies in south-central Texas, USA, within approximately 29.1°N to 31.0°N and 97.4°W to 100.4°W. The total aquifer's surface is 15,650 km², divided into 2,820 km² and 12,830 km² of recharge and confined (discharge) areas, respectively. Ground-water recharge takes place almost exclusively as stream seepage within the recharge area, in stream reaches underlain by the karstified Edwards limestone formation (Puente 1978).

Figure 3 shows the time series of annual ground-water recharge, pumping, and spring flow in the Edwards Aquifer from 1934 to 1995. Spring flow occurs in the discharge zone in a series of large springs (average daily spring flow is on the order of 420×10^3 m³) that support an important and threatened ground-water ecosystem (Longley 1981; U.S. Fish and Wildlife Service 1996). Figure 3 shows that ground-water recharge fluctuates considerably from year to year, ranging from close to zero during drought (see circa 1957) to over 3×10^9 m³ yr⁻¹ in wet years. The recharge time series in Figure 3 suggests an increasing variability of annual recharge over time, although its annual mean of 0.83×10^9 m³ yr⁻¹ remained stable during the monitoring period. The years between 1947 and 1959 were the driest in record. Ground-water pumping has increase since the 1930s; it currently averages between 0.50 and 0.55×10^9
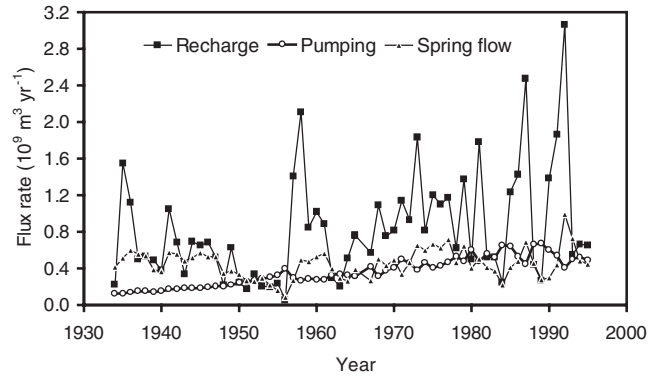

Figure 3. Annual ground-water recharge, pumping, and spring flow in 10^6 m³ in the Edwards Aquifer, 1934–1995.

m³ yr⁻¹. Spring flow follows the general pattern of recharge, but lags it by several months.

Ground-Water Storage Dynamics and Long-Term Aquifer Yield

Figure 4 shows the change in ground-water storage, S, in the Edwards Aquifer from 1934 to 1995. The change in ground-water storage (ΔS) was calculated with the following equation:

$$\Delta S = S(t) - S(1934) = \sum_{1934}^{t} [R(t) - G(t) - W(t)] \quad (8)$$

in which S(1934) is the 1934 storage and G(t), R(t), and W(t) are the annual spring flow, recharge, and pumping at time t, respectively. S(t) is the storage in year t. Figure 4 shows that between 1936 (point A) and 1956 (point B), aquifer storage declined 3.5×10^9 m³ due to pumping and drought. Between 1956 and 1992 (point C) storage recovered 5.1×10^9 m³ in spite of a
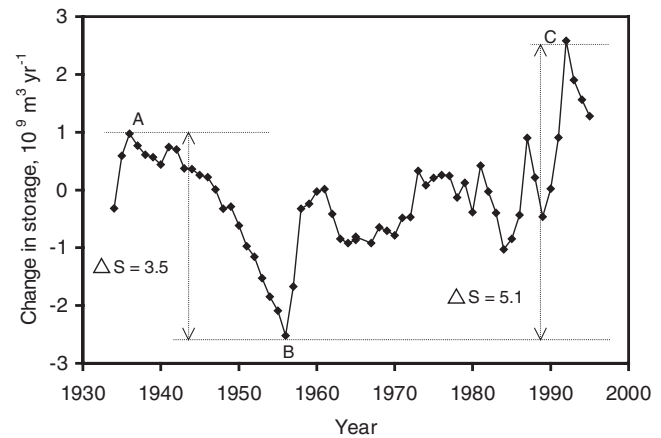

Figure 4. Change in Edwards Aquifer storage, 1934–1995.

steady increase in pumping (see Figure 3). The observed recovery was caused by large-scale recharge following intense rainfall events (most of them associated with the El Niño climatic anomaly). The Edwards Aquifer storage was near its lowest usable limit in 1956. This was corroborated by the drying up of most springs that depended on the aquifer's ground-water storage. The 1992 groundwater levels, on the other hand, were the highest in the historical record. It can be concluded that the Edwards Aquifer's usable storage is approximately 5.1×10^9 m³.

Aquifer storage and long-term aquifer yield (the average annual pumping rate) are interdependent. Graphing the cumulative annual recharge—defined as the sum of annual recharge from 1934 to any subsequent year t—versus time (as is shown in Figure 5) and drawing the minimum-slope tangent that subtends an usable aquifer storage equal to 5.1×10^9 m³ (drawn through point A in Figure 5) produces a theoretical long-term aquifer yield equal to 0.7×10^9 m³ yr^{-1}. The aquifer yield estimated from the cumulative recharge and usable aquifer storage, however, may cause adverse ecological impacts, especially during dry years. When aquifer recharge is below average, spring flow may fall below an ecologically threatening threshold (stress threshold). To avoid those adverse impacts, one must adjust the pumping rate to the fluctuations in recharge caused by climate variation and, hypothetically, by climate change, as shown in the next section of this article.

Spring-Flow Vulnerability to Ground-Water Pumping in a 2xCO$_2$ Climate

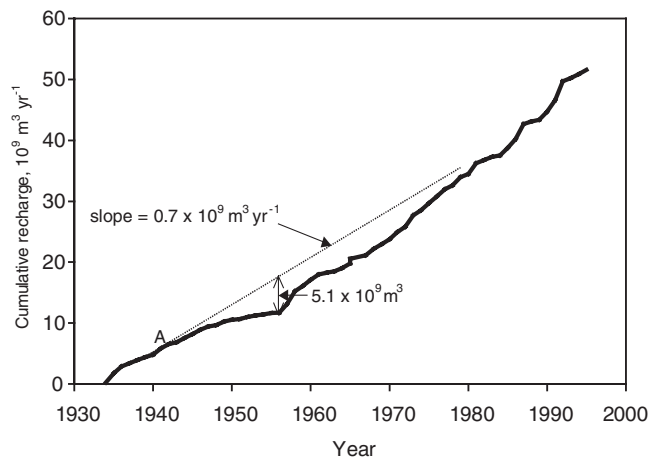The lateral dimensions of the Edwards Aquifer are several orders of magnitude larger than the vertical

Figure 5. Cumulative recharge and estimation of long-term aquifer yield.

dimension. Therefore, ground-water flow and chemical transport were modeled by the following two-dimensional equations:

$$\frac{\partial\left(T(x, y)\frac{\partial h}{\partial x}\right)}{\partial x} + \frac{\partial\left(T(x, y)\frac{\partial h}{\partial y}\right)}{\partial y}$$
$$= S(x, y)\frac{\partial h}{\partial t} + N(x, y) \qquad (9)$$

where h is hydraulic head (dimensions of L), N is the net ground-water flux per unit area (L t^{-1}; N includes recharge, pumping, and spring flow, in general), S is the storage coefficient (dimensionless), T is the transmissivity (L^2 t^{-1}), and t denotes time; and

$$\frac{\partial C}{\partial t} = \frac{\partial\left(D_{ij}\frac{\partial C}{\partial x_i}\right)}{\partial x_i} - \frac{\partial(v_i C)}{\partial x_i} - Z(x, y) \quad i, j = 1, 2 \quad (10)$$

where C is solute concentration (M L^{-3}), D_{ij} is the coefficient of hydrodynamic dispersion (L^2 t^{-1}), Z is the solute flux via ground-water recharge or ground-water pumping (ML^{-3} t^{-1}), and v_i is the average velocity of ground water (L t^{-1}).

Equations (9) and (10) were solved by means of a finite-difference ground-water/transport model called GWSIM IV (Thorkildsen and McElhaney 1992), specifically developed for and calibrated to the Edwards Aquifer. The 2xCO$_2$ climate forcing was created from the VEMAP database scaling factors cited earlier. Specifically, the 2xCO$_2$ ground-water recharge was calculated according to Equation (7), which was, in conjunction with historical and projected ground-water pumping data, used to simulate ground-water levels and spring flow with the numerical ground-water model, GWSIM IV. Water-quality impacts were found to be minor and will not be discussed further here. The climate-change simulations considered the scaling of historical dry and average climate to a warmer (2xCO$_2$) climate by means of the scaling technique described above.

Figure 6 shows typical results of spring-flow response to climate and ground-water use changes in the study area. A wide range of pumping rates was considered in the simulation of the Edwards Aquifer under an "average-climate" 2xCO$_2$ forcing. Annual pumping varied between 0 and 0.784×10^9 m³, where the latter value corresponds to the predicted ground-water use by 2050 in the Edwards Aquifer (Texas Water Development Board 1997). The average-climate 2xCO$_2$ forcing scenario was created by scaling historical aquifer recharge in a period of average recharge (i.e., 1978–1989 in the Edwards aquifer, during which average annual recharge was 0.949×10^9 m³) according to Equation (7). Figure 6 graphs the effect of

ground-water pumping on the two largest springs in the Edwards Aquifer, the San Marcos and Comal springs. It shows that monthly spring flow at the San Marcos Springs is maintained at or above the allowable minimum (called the stress threshold in Figure 6 and equal to 0.73×10^6 m^3 month^{-1}) as long as the pumping rate is less than approximately 0.2×10^9 m^3 yr^{-1}, while the minimum spring flow at the Comal Springs is guaranteed for pumping rates less than 0.68×10^9 m^3 yr^{-1}. Given that the spring flow at San Marcos has low sensitivity to the pumping rate, a compromise pumping rate can be set anywhere between 0.2×10^9 m^3 yr^{-1} and 0.4×10^9 m^3 yr^{-1} without inflicting undue stress on the aquifer ecosystem, provided that recharge is average. Notice that this recommended range of annual pumping under average climatic conditions does not include the long-term aquifer yield estimated in Figure 5 from the long-term cumulative recharge and the usable aquifer storage. The theoretical long-term aquifer yield was estimated at 0.7×10^9 m^3 yr^{-1}, which is on the high side and certain to cause adverse ecological effects.

The results shown in Figure 6 correspond to an average 2xCO$_2$ climatic forcing. Under drought conditions, the pumping strategy must be adjusted. Drought conditions prevailed in the period between 1947 and 1959. A "dry-climate" 2xCO$_2$ forcing was created by scaling the 1947–1959 historical recharge (the annual mean of which was 0.553×10^9 m^3) with the runoff scaling factors (recall equation [7]). The Edwards Aquifer was simulated with the dry-climate 2xCO$_2$ recharge and annual pumping rates that ranged between zero and 0.784×10^9 m^3, the same range used in the average-climate 2xCO$_2$ scenario previously discussed. 7 presents the results. It shows that the San Marcos spring flow falls below the stress threshold regardless of the pumping rate. The Comal spring flow declines steadily with increasing pumping rate. It falls below the stress threshold when the pumping rate exceeds
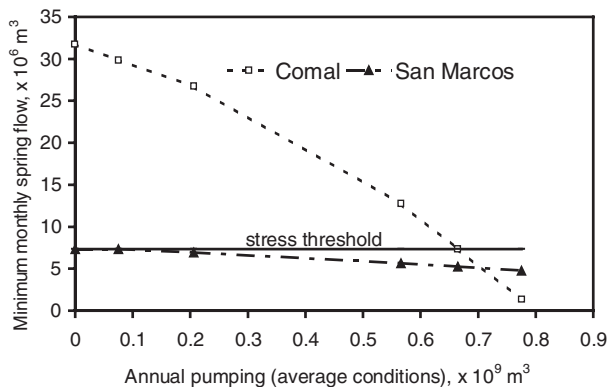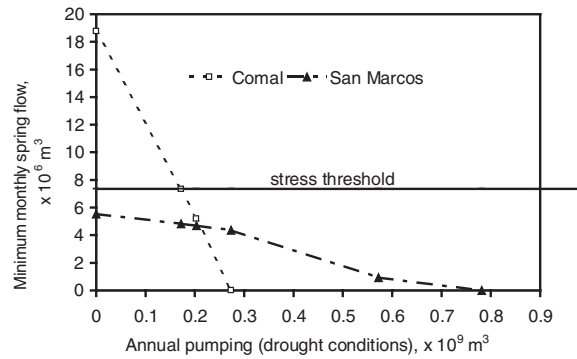

Figure 7. Sensitivity of monthly spring flows to pumping rate under "dry-climate" 2xCO$_2$ scenario in the Edwards aquifer.

0.17×10^9 m^3 yr^{-1}. During protracted droughts, such as that between 1947 and 1959 in the Edwards Aquifer, the competition between human water use and environmental needs is sharply accentuated. In such an instance, one could argue for a range of the annual pumping rate between zero and, say, 0.2×10^9 m^3 yr^{-1}. This type of decision, however, belongs in the realm of politics, where all constituencies are weighed in a comprehensive decision-making framework.

Climate and Ground-Water Use Effects on Hydrologic Response

Let Z denote the level of hydrologic response caused by human use of ground water (W, the ground-water pumped from an aquifer) and by climate (C). Hydrologic response is defined in terms of a specific variable of interest, such as spring flow from an aquifer system (see example below). Z is then a function (f) of W and C, given aquifer properties (denoted by T). Hence, $Z = f(W, C)|_T$ —that is, the function f is conditioned on aquifer properties T. For simplicity, this is written henceforth as $Z = f(W, C)$. A change in hydrologic response, ΔZ, is then related to change in ground-water use (ΔW, caused by population growth and/or economic development) and to climate change (ΔC, due to increased greenhouse gases and aerosols) by the following equation:

$$\Delta Z = \frac{\partial f}{\partial W} \Delta W + \frac{\partial f}{\partial C} \Delta C \qquad (11)$$

The first term on the right-hand side of Equation (11) denotes the change in hydrologic response caused by a change in human use of ground-water while the climate is kept constant. The second term on the right-hand side of Equation (11) represents the change in hydrologic response exerted by climate change while ground-water use remains constant. The following subsection presents

Figure 6. Sensitivity of monthly spring flows to pumping rate under an "average-climate" 2xCO$_2$ scenario in the Edwards aquifer.

Table 1. Climate- and Ground-Water-Use-Change Scenarios Considered in the Analysis of Hydrologic Response

	Scenario			
	Base: I	Climate-Change Effect: II	Effect of Change in Ground-Water Use: III	Total Effects: IV
Climate (recharge)	$R_{1978-1989}$[a]	$R_{1978-1989} \cdot \frac{2xCO_2}{1xCO_1}$[b]	1978–1989 use[c]	$R_{1978-89} \cdot \frac{2xCO_2}{1xCO_1}$
Ground-water use	1978–1989 use	1978–1989 use	2050 use[d]	2050 use

[a] Historical recharge during 1978—1989, the mean of which = 0.949×10^9 m^3 yr^{-1}.
[b] This is the historical recharge scaled to $2xCO_2$ conditions according to equation (7).
[c] The average ground-water use between 1978 and 1989 = 0.567×10^9 m^3 yr^{-1}.
[d] The ground-water use forecast for 2050 = 0.784×10^9 m^3 yr^{-1}.

an example of the quantification of total hydrologic response (i.e., that caused by change in both ground-water use and climate change) and partial hydrologic response (i.e., that caused by either change in ground-water use or climate change).

The evaluation of climate-change and ground-water use effects on hydrologic response suggested by Equation (11) is hindered by the fact that the response function f(W,C) is unknown. Therefore, an approximate method is called for to estimate those effects separately. Table 1 illustrates the scenarios considered in the estimation of ground-water use and climate-change effects. The second column of Table 1 contains the base scenario (scenario I), that in which average climatic conditions—and thus, recharge—prevailed, a situation that took place between 1978 and 1989 (average annual recharge in that period was 0.949×10^9 m^3 and average annual ground-water use was 0.567×10^9 m^3 yr^{-1}). The third column in Table 1 shows the climate-change scenario (scenario II), whereby the historical recharge (1978–1989) was scaled to $2xCO_2$ recharge conditions according to Equation (7) and the ground-water use was kept at the 1978–1989 historical level. The fourth column of Table 1 outlines the change in ground-water use scenario (scenario III), wherein the recharge was kept at the 1978–1989 historical level and ground-water use was set equal to 0.784×10^9 m^3 yr^{-1}, the forecast for 2050 associated with future use in a warmer ($2xCO_2$) climate. The fifth column displays the total-effects (climate-change and ground-water-use) scenario (scenario IV), in which recharge and ground-water use correspond to the hypothesized $2xCO_2$ conditions.

Table 2 summarizes the partial and total-effects results concerning spring flow in the Edwards Aquifer. In the Comal Springs (column 2), the rise in minimum spring flow calculated with scenario II ($2xCO_2$ recharge and base ground-water use) relative to the base scenario I establishes that climate change *increases* spring flow when other things are kept constant. The calculated spring-flow augmentation was from 4.84×10^6 m^3 to 12.7×10^6 m^3—a 162-percent increase in spring flow caused by

climate change. Scenario III (base climate and year-2050 ground-water use) shows that the effect of year-2050 ground-water use is to dry up Comal Springs (i.e., a 100 percent reduction in spring flow), provided that the climate does not change. When the climate and ground-water use changes are considered together (scenario IV), the role of ground-water use over climate change prevails: Comal Springs flow is reduced to 1.31×10^6 m^3 from the 4.84×10^6 m^3 level in scenario I (a 73-percent reduction in spring flow).

Table 2 reveals a similar—albeit attenuated—pattern in minimum spring flow for the San Marcos Springs. It shows that climate change (scenario II) *increases* spring flow relative to the base condition (scenario I) by 17 percent (from 4.84×10^6 m^3 to 5.67×10^6 m^3), while the year-2050 ground-water use (scenario III) reduces spring flow relative to the base condition by approximately 22 percent (from 4.84×10^6 m^3 to 3.79×10^6 m^3). The combined effect of climate change and year-2050 ground-water use is a 1 percent drop in spring flow compared with the base condition (from 4.84×10^6 m^3 to 4.79×10^6 m^3): here, too, ground-water use dominates over climate change in this instance.

The results indicate, therefore, that the primary threat to ground-water use in the Edwards Aquifer comes from

Table 2. Minimum Spring Flow in the Edwards Aquifer Caused by Climate-Change and Ground-Water-Use Scenarios

Climate-Change and Ground-Water-Use Scenario[a]	Edwards Aquifer Springs	
	Comal	San Marcos
I	4.84	4.84
II	12.7 (+162%)[b]	5.67 (+17%)
III	0 (−100%)	3.79 (−22%)
IV	1.31 (−73%)	4.79 (−1%)

Note: Spring flow is in 10^6 m^3 month^{-1}.
[a] The scenarios are the same ones defined in Table 1.
[b] The numbers within parentheses represent the percentage increase (+) or decrease (−) caused by a scenario relative to the base condition (I).

the rise in ground-water use associated with predicted growth, not from climate change. The latter, in fact, would increase spring flow in the study area.

Summary

This article summarized the theory of climate change and the relationship of climate-change forcing to hydrologic processes. The article focused on regional aquifer systems and on the methods used to link large-scale climate-change processes to ground-water recharge, ground-water flow, and solute transport in a warmer climate. There are substantial uncertainties associated with climate-change scenarios, be they transient or equilibrium $2xCO_2$ cases. Those uncertainties stem primarily from the complexity of the earth's climate system and from complex, nonlinear climate feedbacks that arise in connection with a warming planet. The article reviewed methods currently available to generate climate-change scenarios and to simulate regional aquifer systems under those scenarios. It introduced a methodology to calculate the effects of climate change and population growth on hydrologic response. The Edwards Aquifer of Texas, one of the largest fresh-water aquifers in the U.S., was used to illustrate a specific procedure and our current capabilities to assess the potential impacts of a warming climate and changes in ground-water use on regional-scale aquifer systems. Results indicate that aquifer exploitation strategies must be adapted to climate variability and climate change. In particular, protracted drought sharply accentuates the competition between human and ecological water uses. It was also determined that changes in ground-water use by population growth may cause more profound aquifer impacts than those associated with global warming.

Acknowledgments

Notes

1. A summary of climate-change science may be found in the 2001 report by the Intergovernmental Panel for Climate Change (IPCC) on its Web site.
2. See Loáiciga, Maidment, and Valdes (2000) for a list of GCMs used in hydrologic studies. See http://www. mmm.ucar.edu/mm5/mm5-home.html for a description of the RCM MM5 (Mesoscale Model 5) of the National Center for Atmospheric Research, US.
3. GCM-RCMs yield runoff-scaling ratios rather than stream-flow ratios, but when averaged over relatively large areas, these two ratios converge to the same value. Runoff in GCM-RCMs is equal to the land-based water flux from model cells, while stream-flow is defined in hydrology as the sum of overland flow, interflow, and baseflow concentrated in the stream channel.

References

Demeritt, D. 2001. The construction of global warming and the politics of science. *Annals of the Association of American Geographers* 91 (2): 307–37.

Forest, C. E., H. P. Stone, A. P. Sokolov, M. R. Allen, and M. D. Webster. 2002. Quantifying uncertainties in climate system properties with the use of recent climate observations. *Science* 295: 113–16.

Giorgi, F., M. R. Marinucci, and G. T. Bates. 1993a. Development of a second-generation regional climate model (RegCM2). Part 1: Boundary layer and radiative transfer processes. *Monthly Weather Review* 121: 2794–813.

Giorgi, F., M. R. Marinucci, and G. T. Bates. 1993b. Development of a second-generation regional climate model (RegCM2). Part 2: Convective processes and lateral boundary conditions. *Monthly Weather Review* 121: 2814–32.

Giorgi, F., C. Shields-Brodeur, and G. T. Bates. 1994. Regional climate change scenarios over the United States produced with a nested regional climate model. *Journal of Climate* 7: 375–99.

Gleick, P. 1989. Climate change, hydrology, and water resources. *Reviews of Geophysics* 27 (3): 329–44.

Hansen, J., R. Ruedy, M. Sato, and K. Lo. 2002. Global warming continues. *Science* 295: 275.

Hargreaves, G. H., and Z. A. Zamani. 1982. Estimating potential evapotranspiration. *Journal of Irrigation and Drainage Engineering* 108 (3): 225–30.

Henderson-Sellers, A., and A. J. Pitman. 1992. Land-surface schemes for future climate models: Specification, aggregation, and heterogeneity. *Journal of Geophysical Research* 97 (D3): 2687–96.

Houghton, J. T., Filho L G. Meira, B. A. Callander, N. Harris, A. Kattenberg, and K. Maskell. 1996. *Climate change 1995: The science of climate change.* Cambridge, U.K.: Cambridge University Press.

Intergovernmental Panel for Climate Change (IPCC). 2001. Report. htpp://www.ipcc.ch (last accessed 30 October 2002).

Kerr, R. 1994. Climate modeling's fudge factor comes under fire. *Science* 265: 1528.

———. 1997. Greenhouse forecasting still cloudy. *Science* 276: 1040–42.

Kittel, T. G. F., N. A. Rosenblum, T. H. Painter, and D. S. Schimel. 1995. VEMAP modeling participants, the VEMAP integrated database for modeling United States ecosystem/vegetation sensitivity to climate change. *Journal of Biogeography* 22: 857–62.

Lindzen, R. S. 1990. Some coolness concerning global warming. *Bulletin American Meteorological Society* 71: 288–99.

Loáiciga, H. A. 1997. Runoff scaling in large rivers of the world. *The Professional Geographer* 49 (3): 356–63.

———. 2000. Climate-change impacts in regional-scale aquifers: Principles and field application. In *Ground water updates*, ed. K. Sato and Y. Iwasa, 247–52. Tokyo: Springer-Verlag.

Loáiciga, H. A., L. Haston, and J. Michaelsen. 1993. Dendrohydrology and long-term hydrologic phenomena. *Reviews of Geophysics* 31 (2): 151–71.

Loáiciga, H. A., and R. B. Leipnik. 2000. Closed-form solutions to aquifer management. *Journal of Water Resources Planning and Management* 126 (1): 30–35.

Loáiciga, H. A., D. R. Maidment, and J. B. Valdes. 2000. Climate-change impacts in a regional karst aquifer, Texas, USA. *Journal of Hydrology* 227: 173–94.

Loáiciga, H. A., D. R. Maidment, J. B. Valdes, M. Roos, and E. F. Wood. 1996. *River basins vulnerable to global warming.* Report of the ASCE/USEPA Case Studies Team. Reston, VA: American Society of Civil Engineers.

Loáiciga, H. A., J. B. Valdes, R. Vogel, J. Garvey, and H. H. Schwarz. 1996. Global warming and the hydrologic cycle. *Journal of Hydrology* 174 (1–2): 83–128.

Longley, G. 1981. The Edwards aquifer: Earth's most diverse ground-water ecosystem. *International Journal of Speleology* 11: 123–28.

Lorenz, E. 1963. Deterministic non-periodic flow. *Journal of Atmospheric Sciences* 20: 130–41.

———. 1967. The predictability of a flow which possesses many scales of motion. *Tellus* 21: 289–307.

Maclay, R. W., and T. W. Small. 1984. *Carbonate geology and hydrology of the Edwards aquifer, San Antonio area.* Open File Report 83–537. Austin, TX: United States Geological Survey.

Mitchell, J. F. B., T. C. Jones, J. M. Gregory, and S. F. B. Tett. 1995. Climate response to increasing levels of greenhouse gases and sulphate aerosols. *Nature* 376: 501–4.

National Center for Atmospheric Research. http://www.mmm.ucar.edu/mm5/mm5-home.html (last accessed 30 October 2002).

Panagoulia, D. 1992. Impacts of GISS-modeled climate changes in catchment hydrology. *Hydrologic Sciences Journal* 37 (2): 141–63.

Puente, C. 1978. *A method of estimating natural recharge in the Edwards aquifer in the San Antonio area, Texas.* Water Resources Investigations Report no. 78–10. Austin, TX: United States Geological Survey.

Ramanathan, V., and W. Collins. 1992. Thermostat and global warming. *Nature* 357: 649–53.

Stone, D. B., C. L. Moomaw, and A. Davis. 2001. Estimating recharge distribution by incorporating runoff from mountainous areas in an alluvial basin in the Great Basin region of the southwestern United States. *Ground Water* 39 (6): 807–18.

Texas Water Development Board. 1997. *Water for Texas: A consensus-based update to the state's water plan.* Vol. 2, *Technical planning appendix.* Document GP–6–2. Austin, TX: Texas Water Development Board.

Thorkildsen, D., and P. D. McElhaney. 1992. *Model refinement and applications for the Edwards BFZ aquifer in the San Antonio region, Texas.* Report 340 Austin, TX: Texas Water Development Board.

Thornthwaite, C. W. 1948. An approach toward a rational classification of climate. *Geographical Review* 38: 1–55.

U.S. Fish and Wildlife Service. 1996. *San Marcos and Comal Springs and associated ecosystems (revised) recovery plan.* Austin, TX: Austin Ecological Services Station, United States Fish and Wildlife Service.

Vaccaro, J. J. 1992. Sensitivity of ground water recharge estimates to climate variability and change, Columbia Plateau, Washington. *Journal of Geophysical Research* 97 (D3): 2821–33.

Vegetation Ecosystem Modeling and Analysis Project (VEMAP). Database. http://www.cgd.ucar.edu/vemap (last accessed 30 October 2002).

Waterloo Hydrogeologic. Visual Modflow. http://www.flowpath.com/software/visualmodflow/visualmodflow.html#top (last accessed 30 October 2002).

Vörösmarty, C. J., P. Green, J. Salisbury, and R. B. Lammers. 2000. Global water resources: Vulnerability from climate change and population growth. *Science* 289: 284–88.

Correspondence: Department of Geography, University of California, Santa Barbara, CA 93106-4060 USA; e-mail: hugo@geog.ucsb.edu.